Analytical Biochemistry 660 (2023) 114929

Contents lists available at ScienceDirect

Analytical Biochemistry

journal homepage: www.elsevier.com/locate/yabio

Protein A–Nanoluciferase fusion protein for generalized, sensitive detection of immunoglobulin G

Suman Nandy [a], Mary Crum [a,1], Katherine Wasden [a,2], Ulrich Strych [a,3], Atul Goyal [a,4], Vijay Maranholkar [b], William Mo [a,5], Binh Vu [a], Katerina Kourentzi [a], Richard C. Willson [a,b,c,*]

[a] William A. Brookshire Department of Chemical and Biomolecular Engineering, University of Houston, Houston, TX, USA
[b] Department of Biology and Biochemistry, University of Houston, Houston, TX, USA
[c] Escuela de Medicina y Ciencias de Salud, Tecnológico de Monterrey, Monterrey, Nuevo León, Mexico

ARTICLE INFO

Keywords:
Protein A
Nanoluciferase
Bioluminescence
IgG detection
SARS-CoV-2 Nucleoprotein
Immunoassay

ABSTRACT

Detection and quantification of antibodies, especially immunoglobulin G (IgG), is a cornerstone of ELISAs, many diagnostics, and the development of antibody-based drugs. Current state-of-the-art immunoassay techniques for antibody detection require species-specific secondary antibodies and carefully-controlled bioconjugations. Poor conjugation efficiency degrades assay performance and increases the risk of clinical false positives due to non-specific binding. We developed a generic, highly-sensitive platform for IgG quantification by fusing the IgG-Fc binding Z domain of Staphylococcal Protein A with the ultrabright bioluminescence reporter Nanoluc-luciferase (Nluc). We demonstrated the application of this fusion protein in a sandwich IgG detection immunoassay using surface-bound antigens to capture target IgG and protein A-Nanoluc fusion as the detector. We optimized the platform's sensitivity by incorporating multiple repeats of the Z domain into the fusion protein constructs. Using rabbit and mouse anti-SARS-CoV-2 Nucleoprotein IgGs as model analytes, we performed ELISAs in two different formats, either with SARS-CoV-2 Nucleoprotein as the capture antigen or with polyclonal chicken IgY as the capture antibody. Using standard laboratory equipment, the platform enabled the quantitation of antibody analytes at concentrations as low as 10 pg/mL (67 fM).

1. Introduction

Detection of antibodies is essential to many biomedical assays, diagnostics, and in the development of antibody-based drugs, the fastest-growing class of biopharmaceuticals. Current antigen and antibody detection methods usually involve a labeled detector, commonly a secondary antibody conjugated with a reporter enzyme, fluorophore, nanoparticle, DNA, or electrochemically-active species. These and many emerging antibody labeling techniques, such as carbon dot-based fluorescence immunoassay [1] and graphene quantum dot-labeled luminescence resonance energy transfer assay [2], rely heavily on carefully-prepared secondary antibody–reporter conjugates. Most antibody detection platforms utilize maleimide–thiol coupling chemistries [3], cysteine-based native chemical ligation [4,5], or carbodiimide or N-hydroxysuccinimide (NHS) chemistries [6] to prepare the secondary antibody–reporter conjugate. A drawback of these approaches is that heterogeneous coupling of the secondary antibody–reporter conjugate can reduce the analytical and diagnostic utility of the detection assay.

Proteins that bind the antibody Fc fragment are widely used in antibody purification, especially *Staphylococcus aureus* protein A (SpA) [7], a cell wall-anchored virulence factor that promotes *S. aureus* pathogenicity. The SpA contains five homologous IgG-binding domains (E, D, A, B, and C), with the B domain widely used as an affinity purification ligand for antibodies and Fc-containing recombinant proteins. The B domain binds to the IgG-Fcγ [8], primarily through interaction with nine conserved hydrophobic residues between the C_H2 and C_H3 [9–11]. This

* Corresponding author. William A. Brookshire Department of Chemical and Biomolecular Engineering, University of Houston, Houston, TX, USA.
E-mail address: willson@uh.edu (R.C. Willson).
[1] Present address: Department of Molecular and Human Genetics, Baylor College of Medicine, Houston, TX, USA.
[2] Present address: Harvard Medical School, Boston, MA, USA.
[3] Present address: Department of Paediatrics, National School of Tropical Medicine, Baylor College of Medicine, Houston, TX, USA.
[4] Present address: Vaccine Research and Development, Pfizer, Pearl River, NY, USA.
[5] Present address: Department of Biomedical Engineering, The University of Texas at Austin, TX, USA.

https://doi.org/10.1016/j.ab.2022.114929
Received 20 June 2022; Received in revised form 7 September 2022; Accepted 20 September 2022
Available online 19 October 2022

domain was later subjected to site-specific mutagenesis to produce the more stable Z domain (Ala1Val and Gly29Ala) [12], where the substitutions lie outside the α-helical IgG contact regions and so do not interfere with IgG binding [12]. Multimers of the Z domain have much higher affinity than the monomeric Z domain [13] because of their significantly lower dissociation rate constants; for example, the k_{off} is 3.2×10^{-3} s^{-1} for the monomeric Z domain and 0.51×10^{-3} s^{-1} for dimeric Z domain [14,15]. In previous work, we successfully employed fluorescein-labeled oligomers of the Z domain in real-time detection of human IgG using shifts in fluorescence polarization and intensity upon IgG binding [16]. Previous studies reported the analytical application of firefly and bacterial luciferases [17–19], genetically fused with protein A, as universal bioluminescent antibody detectors, but observed a high detection limit (10 ng/ml [17]) and reduced luciferase activity (10%–50%) [19,20]. Later approaches to improving reporter performance included amino acid mutations [21], replacement of protein A with streptococcal protein G [22], and fusion of an Fc-binding peptide with *Renilla* luciferase instead of firefly luciferase [23]. However, irreversible denaturation and proteolytic cleavage of fusion protein [20] impaired their wide acceptance.

Nanoluc® luciferase (Nluc) is a small (171 amino acids, 19.2 kDa), monomeric, highly-stable, ATP-independent luciferase [24] that produces an extremely bright sustained bioluminescence with the coelenterazine derivative furimazine with specific activity 150 times higher than that of any other luciferase [24]. Despite having a non-ideal emission maximum (460 nm), at which many biological samples have either high absorbance or autofluorescence [25], Nluc is widely used for molecular imaging and detection of disease markers [25–27]. In this work, we fused the gene encoding Nluc with three or five repeats of the Z-domain gene and a His_6 tag to produce recombinant Z3-Nluc and Z5-Nluc proteins, respectively, for sensitive detection of IgG. After confirming the sequences of the genetic constructs, we purified the recombinant fusion proteins on IgG Sepharose and Ni-NTA columns and characterized the proteins by SDS-PAGE and MALDI-ToF mass spectrometry. We then demonstrated the use of these proteins in the detection of SARS-CoV-2 Nucleoprotein (NP)-specific IgGs in sandwich ELISA format using either plate-immobilized NP as capture antigen or using polyclonal chicken IgY (which is not bound by protein A [28,29]) as capture antibody.

2. Materials and methods

2.1. Materials

Synthetic nucleic acids were obtained from Integrated DNA Technologies (IA, USA). Triton X-100, bovine serum albumin (BSA), chicken egg-white lysozyme, Benzonase® Endonuclease, LB broth (Miller), IPTG, Tris, DTT, imidazole, and Amicon centrifugal filters were purchased from Sigma (MO, USA). Pierce™ Protease Inhibitor Mini Tablets EDTA-free, SYBR green I, Pierce™ BCA Protein Assay Kit, and Zeba™ Spin Desalting Columns were purchased from Thermo Fisher Scientific (MA, USA). Other reagents used were glacial acetic acid, sodium hydroxide, hydrochloric acid (Macron, KY, USA), anhydrous ethanol (VWR, PA, USA), and PBS tablets (Takara Bio, CA, USA). Buffers were prepared with deionized water (Millipore Milli-Q, USA) and filtered with sterile polystyrene filters (Corning, NY, USA). Gibson Assembly® Cloning Master Mix (GA), Nanoglo™ assay substrate (N112A), restriction enzymes, and Q5® High-Fidelity polymerase 2X Master Mix were purchased from Promega (WI, USA) or New England Biolabs (MA, USA). QIAprep Spin Miniprep, QIAquick Gel Extraction, polymerase chain reaction (PCR) cleanup, and plasmid miniprep kits were purchased from Qiagen (MD, USA). IgG Sepharose 6 Fast Flow, Ni Sepharose 6 Fast Flow resins, and XK 16/20 columns were purchased from Cytiva (MA, USA) or (GE Healthcare Life Sciences, IL, USA). Transformation-competent *Escherichia coli* BL-21(DE3) cells and pET plasmids were obtained from Invitrogen (MA, USA). PCR was carried out in an MJ Mini Thermal Cycler (Bio-Rad Laboratories, CA, USA). The buffer used to determine the activity of Nluc (Nbuffer) was prepared with 100 mM MES, 1 mM CDTA (cyclohexanediaminetetra-acetic acid), 0.5% (v/v) Tergitol, 150 mM KCl, and 1 mM DTT, pH 6.0 as reported previously [24]. 96-well white flat-bottom polystyrene high-binding and medium-binding microplates were purchased from Corning (NY, USA) and Greiner Bio-One (NC, USA), respectively. TST buffer was 50 mM Tris, 150 mM NaCl, and 0.05% Tween 20, pH 7.8. PBST buffer was PBS +0.05% Tween 20, pH 7.4. The assay diluent buffer was PBST +0.1% BSA. Microplate coating buffer was 0.05 M sodium bicarbonate, and 0.05 M sodium carbonate, pH 9.5.

2.2. Construction of Z-Nluc genes and plasmids

A synthetic gene encoding the Z domain was prepared in a pUC57-Amp vector by Genewiz (South Plainfield, NJ, USA). Genes encoding Z domain trimer and pentamer, Z3 and Z5, respectively, were amplified from the previously reported plasmids, pET28a-3Z and pET28a-5Z (see supplementary section SI 1.1), using a high-fidelity DNA polymerase (Q5® High-Fidelity 2X Master Mix) and primers *Nde*I-N-Z-F (5′-CTGGTGCCGCGCGGCAGCCATAT-3′)/Z-Nluc-R (5′-GAAAGTCGACTTACAAGCTGGCATGGTTTTCACCCTGGAAGACTTC-3′). The synthetic DNA fragment encoding Nluc was PCR-amplified from the previously reported plasmid, pET28a-NanoLuc, using primers Z-Nluc-F (5′-GAAGTCTTCCAGGGTGAAAACCATGCCAGCTTGTAAGTCGACTTTC-3′)/*Xho*I-Nluc-R (5′-GGTGGTGGTGGTGCTCGAG-3′). PCR fragments were analyzed by gel electrophoresis and visualized by SYBR green-staining. Fragments migrating the proper distance on the gels were excised and purified using a QIAquick Gel Extraction Kit. The purified fragments were assembled in an isothermal Gibson Assembly (GA) reaction following the manufacturer's recommended protocol. Briefly, the gel-purified Nluc gene fragment (50 ng/μL) was incubated with that encoding either Z3 or Z5 (25 ng/μL) and 2X GA reaction mix at 50 °C for 2 h. PCR amplification was performed using primers (*Nde*I-N-Z-F/*Xho*I-Nluc-R) with the GA reactions as templates to produce Z3-Nluc and Z5-Nluc genes. Purified gene fragments were incubated with *Nde*I/*Xho*I digested pET28a vector (30 ng/μL) and 2X GA reaction mix at 50 °C for 2 h. Then, 2 μL of the reaction products were transformed into DH5α competent cells and cultured on kanamycin-LB plates overnight at 37 °C. Transformants were then used for PCR amplification with the *Nde*I-N-Z-F and *Xho*I-Nluc-R primer pair. The newly constructed Z-Nluc gene constructs (Z3–6Aalinker–Nluc and Z5–6Aalinker–Nluc) were confirmed by agarose gel electrophoresis. The gene-encoding plasmids, pSNRW-Z3-Nluc and pSNRW-Z5-Nluc, (Supplementary Fig. S1A and Fig. S1B), were then confirmed by Sanger sequencing at Genewiz, with a primer pair corresponding to the T7 promoter (5′-TAATACGACTCACTATAGGG-3′) and T7 terminator (5′-GCTAGTTATTGCTCAGCGG-3′). The sequences were compiled and compared to the designed gene sequences using the MAFFT algorithm in the online tool Benchling (https://benchling.com; see SI section 1.2). Finally, plasmids were purified using a QIAprep Spin Miniprep Kit and transformed into *E. coli* BL-21(DE3) competent cells for high-level protein expression. Plasmids have been deposited and are freely available through the nonprofit Addgene repository (pSNRW-Z3-Nluc: Plasmid #174486; and pSNRW-Z5-Nluc: Plasmid #174487).

2.3. Prediction of Z3-Nluc and Z5-Nluc tertiary structures

The amino acid sequences of the Z domain [30] and Nluc [31] were obtained from the Protein Data Bank (PDB) [32]. The compiled sequences of the Z3-Nluc and Z5-Nluc proteins were submitted to Phyre2 [33] (Protein Homology/analogY Recognition Engine V 2.0, Imperial College, London) for structure prediction by homology modeling and *ab initio* techniques.

2.4. Protein expression

A 5 mL aliquot of freshly-transformed *E. coli* BL-21(DE3) cells in LB medium was incubated for 4–5 h at 37 °C and then transferred to 2.8 L baffled Fernbach flasks containing 500 mL Super Broth (32 g tryptone, 20 g yeast extract, 5 g NaCl, 5 ml 1 N NaOH) with 50 μg/ml kanamycin. When the cultures reached an OD_{600} of 0.6, they were induced with 1 mM isopropyl β-D-1-thiogalactopyranoside (IPTG) and grown for an additional 5 h. Bacterial cells were then harvested in an Avanti J-E High-Speed Centrifuge (Beckman Coulter, CA, USA) at 6000×*g* for 20 min and stored at −20 °C until further use.

2.5. Purification of Z3-Nluc and Z5-Nluc proteins

Frozen cell pellet (10 g) was resuspended in 25 mL lysis buffer (50 mM Tris pH 8.0, 0.1% Triton X-100, 100 μg/ml chicken egg-white lysozyme, 1 tablet of Pierce™ Protease Inhibitor Mini, 2 mM $MgCl_2$), lysed by three passages through a French press (Thermo Electron Corporation, MA, USA) at a working pressure of 20,000 psi, and then centrifuged at 20,000×*g* for 30 min at 4 °C. Hexahistidine-tagged proteins were purified by IgG affinity chromatography and immobilized metal affinity chromatography (IMAC) at 4 °C on an ÄKTA™ UV-900, P-900, pH/C-900, Frac-950 purification system (GE Healthcare Life Sciences, IL, USA). For IgG Sepharose purification, an XK 16/20 column was packed with 5 mL IgG Sepharose 6 Fast Flow resin and equilibrated for 20 min with equilibration buffer (25 mM Tris-HCl, pH 7.8), with all steps performed at a linear flow rate of 100 cm/h. Next, the column was loaded with 25 mL of centrifuged lysate and washed with 10 CV of TST buffer, and the bound proteins were eluted with glycine–HCl buffer (0.1 M, pH 2.9). The peak fractions were collected using a Frac-950 automatic fraction collector with 5 ml tubes containing 2 M Tris for pH neutralization. The protein concentration in each fraction was measured at 280 nm using a NanoDrop™ Spectrophotometer. For IMAC purification, protein-containing fractions were pooled and loaded onto an XK 16/20 Column packed with 5 mL Ni Sepharose 6 Fast Flow, which had been previously equilibrated for 20 min with 50 mL wash buffer (25 mM Tris-HCl, pH 7.8, 20 mM imidazole). The column was then washed with 10 CV of wash buffer, and the bound proteins were eluted with a linear gradient of imidazole from 0 mM to 500 mM in wash buffer over 20 CV. Elution peaks were collected, dialyzed using Amicon 3 kDa MW cutoff centrifugal filters against Tris–HCl buffer (0.02 M, pH 7.5), and stored at −20 °C for later use.

2.6. Protein characterization

SDS-PAGE was performed using Mini-PROTEAN® TGX™ Precast Gels (Bio-Rad, CA, USA), according to the manufacturer's recommendation. All samples for electrophoresis were reduced with 1 M DTT in 2X Laemmli buffer and heated to 95 °C for 5 min. The gel was stained with 0.1% (w/v) Coomassie blue R-250, 20% (v/v) methanol, and 10% (v/v) acetic acid. The molecular weights of the proteins were also confirmed by MALDI-ToF-MS (Voyager STR-DE, Applied Biosystems, MA, USA) analysis at the Tufts University Core Facility (MA, USA). Concentrated protein samples (~5 mg/ml), quantified by Pierce™ BCA Protein Assay Kit, were resuspended by buffer exchange in Tris–HCl buffer (0.02 M, pH 7.5) on a Zeba™ Spin Desalting Column and submitted frozen to the core facility on dry ice. For MW determination, 0.5 μL sample was spotted on a stainless steel plate followed by the addition of 0.5 μL of Sinapinic acid as the matrix. The plate was then air dried, and the mass peaks (m/Z) were detected in linear mode.

2.7. NLuc activity assay

A solution of Nanoglo™ assay substrate diluted in Nbuffer (substrate solution: buffer = 1: 800 by volume) was added to Z–Nluc protein-containing wells of a 96-well white polystyrene high-binding microplate (100 μl per well) and mixed. After briefly shaking (60 s), luminescence was measured in an Infinite® 200 PRO plate reader (Tecan, NC, USA) with a 0.1 s integration time.

2.8. Quantification of IgG using SARS-CoV-2 NP as the capture molecule

For anti-SARS-CoV-2 NP antibody detection, 100 μl of 5 μg/ml recombinant SARS-CoV-2 NP (ACROBiosystems, DE, USA), diluted in coating buffer was added into each well of a white polystyrene high-binding microplate and incubated at 4 °C overnight. After three washes with PBST (HydroFlex microplate washer, Tecan, NC, USA), the wells were passivated with blocking buffer (3% BSA in PBS) for 2 h at 37 °C. Assay standards, controls, and test samples were diluted as needed in the diluent buffer. Then, a 100 μl aliquot of anti-SARS-CoV-2 NP antibodies serially diluted from 1000 ng/ml to 10 pg/ml in diluent buffer was added to wells in duplicate and incubated for 60 min at 25 °C. For no-antibody controls (duplicate), 100 μl PBS containing 0.1% BSA was used. The wells were then washed three times with PBST, and 100 μl of 2 μg/ml recombinant Z–Nluc protein in PBS/0.1% BSA was added per well. After incubation for 60 min at ambient temperature, the plate was washed five times with PBST, and the bound enzyme activity was determined by NLuc activity assay.

2.9. Quantification of IgG using anti-SARS-CoV-2 NP chicken IgY as capture molecule

Here the anti-SARS-CoV-2 NP antibody detection was performed using a chicken anti-SARS-CoV-2 NP IgY polyclonal antibody (Icosagen, CA, USA) as a capture molecule since chicken IgY is not bound by protein A. A white polystyrene high-binding microplate was coated with 5 μg/ml chicken anti-NP IgY in coating buffer and incubated overnight at 4 °C. After three washes with PBST and blocking with 3% BSA in PBS for 2 h at 37 °C, a 100 μl aliquot of 2 μg/ml SARS-CoV-2 NP was added to each well, and the wells were incubated for 1 h at 25 °C. Then, 100 μl aliquots of appropriately diluted assay standard, control solution, and anti-SARS-CoV-2 NP antibodies (serially diluted from 1000 ng/ml to 10 pg/ml) were added to the wells in duplicate and incubated for 60 min at 25 °C. The wells were washed three times with PBST, and 100 μl of 2 μg/ml recombinant Z–Nluc protein was added per well and incubated for 1 h at 25 °C. After incubation for 1 h at ambient temperature, the wells were washed five times with PBST, and the NLuc activity assay determined the activity of the bound enzymes.

2.10. Specific analyte detection in human serum

The Z5-Nluc fusion protein was applied to detect specific IgGs and SARS-CoV-2 NP spiked in human serum. Human serum was obtained from Gulf Coast Regional Blood Center, Houston, TX and stored at −20 °C before the widespread emergence of SARS-CoV-2 virus. Serum was briefly centrifuged and diluted 1:10 in assay diluent to produce 10% human serum. First, a dilution series of SARS-CoV-2 NP spiked in 10% serum was added to chicken anti-SARS-CoV-2 NP IgY-coated wells of a white polystyrene medium-binding microplate. After the wells were washed, 100 μl of 1 μg/ml rabbit anti-SARS-CoV-2 NP IgG was added. The wells were washed, followed by the addition of 2 μg/ml Z5–Nluc protein, and the antibody concentration was determined as described in the previous section. In a separate experiment, 2 μg/ml SARS-CoV-2 NP was incubated in chicken anti-SARS-CoV-2 NP IgY-coated wells of a white polystyrene medium-binding microplate. Next, a dilution series of rabbit anti-SARS-CoV-2 NP IgG spiked into 10% human serum was added to the wells and incubated for 60 min at 25 °C. The wells were washed, followed by the addition of 2 μg/ml Z5–Nluc protein, and the antibody concentration was determined as described above.

2.11. Assay performance metrics

The limit of detection (LOD) of the assay was defined as the lowest analyte concentration for which the average relative luminescence unit (RLU) surpasses the no-analyte/blank RLU value plus three times the standard deviation of the blank. The linear dynamic range was the range of concentrations over which the RLU values are directly proportional to the concentration of the analyte with a correlation coefficient (R^2) >0.95.

3. Results and discussion

3.1. Expression and purification of recombinant Z-Nluc fusion proteins

After the Z3-Nluc and Z5-Nluc gene constructs (Fig. 1A) were cloned and transformed into *E. coli* BL-21(DE3) cells, several kanamycin-resistant transformants were screened by PCR and agarose gel electrophoresis and sequenced by Sanger sequencing. Agarose gel imaging confirmed the presence of the 1101 bp (Fig. 1B) and 1452 bp (Fig. 1C) inserts in the pSNRW-Z3-Nluc and pSNRW-Z5-Nluc plasmids, respectively (Fig. S1A and Fig. S1B). Sanger sequencing confirmed identical sequences of the designed constructs and the sequenced plasmids (see supplementary section SI 1.2). The Phyre2 prediction of the recombinant protein structure predicted helix unwinding in the third Z domain of the Z3-Nluc protein (Fig. 2A) and the fifth Z domain of the Z5-Nluc protein (Fig. 2B). However, successful IgG affinity purification of the Z3-Nluc (Fig. 1D (lane 3) and Fig. S2A) and Z5-Nluc (Fig. 1E (lane 3) and

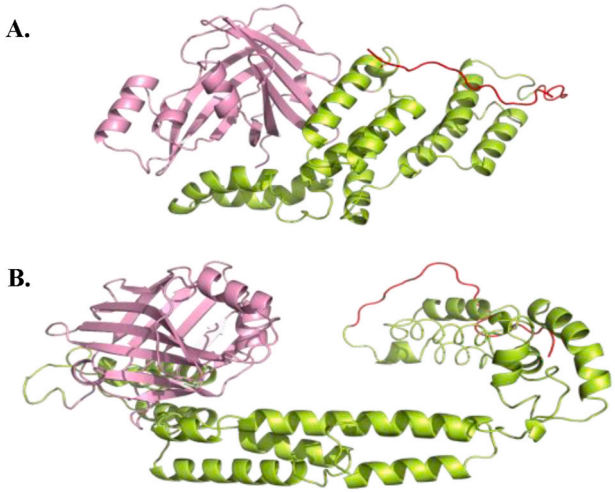

Fig. 2. The predicted tertiary structures of the Z3-Nluc and Z5-Nluc proteins. The Z domain helices are shown in green, the Nluc in pink, and the His_6 tag in red. (A) Z3–Nluc (a single Nluc with three repeats of the Z domain). (B) Z5–Nluc (a single Nluc with five repeats of the Z domain). Loop modeling and sequence alignments were generated using Phyre2 (Protein Homology/analogy Recognition Engine V 2.0, Imperial College, London). The structures were drawn using PyMOL (Schrödinger, Inc, NY, USA). (For interpretation of the references to colour in this figure legend, the reader is referred to the Web version of this article.)

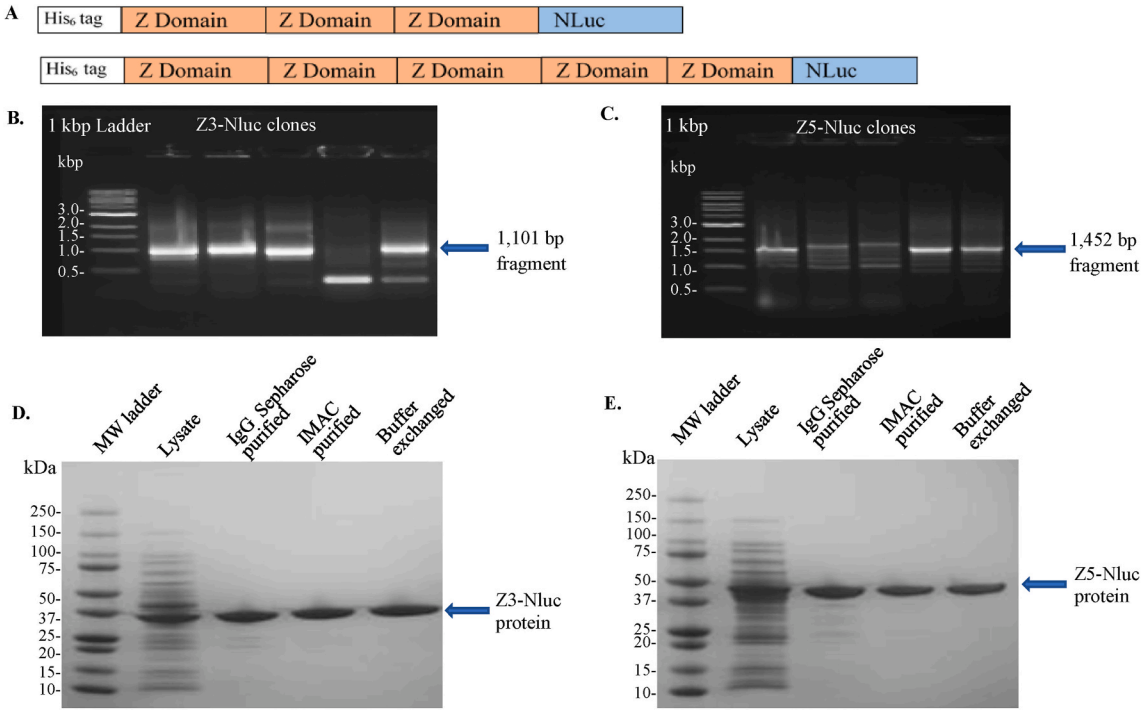

Fig. 1. Gene fragment assembly and recombinant protein characterization. (A) Gene schematics. (B and C) Agarose gel electrophoresis of colony PCR amplicons: five bacterial transformants were selected from LB-kanamycin plates, grown at 37 °C for 4 h, centrifuged briefly to collect the cell pellet which was incubated for 5 min at 98 °C to extract plasmids. PCR amplification of the insert gene fragments was performed with the sequencing primer pair (*Nde*I-N-Z-F, *Xho*I-Nluc-R). After electrophoresis, amplicons were visualized with SYBR green I dye (B) Z3-Nluc and (C) Z5-Nluc transformants. (D and E) SDS-PAGE analysis of IgG affinity and immobilized metal affinity (IMAC) purification fractions of (D) Z3-Nluc and (E) Z5-Nluc protein. (For interpretation of the references to colour in this figure legend, the reader is referred to the Web version of this article.)

Fig. S2B) confirms the proteins possessed a high IgG-affinity. Furthermore, Nluc activity assays on the serially diluted recombinant proteins confirmed that Nluc activity was conserved in each protein, as shown in Fig. S3. Previous reports also show that Nluc well retained enzymatic activity when fused to GFP [34], Protein G [35], or full-length antibodies [36]. Thus, the multistep affinity purification yielded a highly-purified protein (Fig. 1D and E) with luciferase and IgG-binding activity.

3.2. MW confirmation of recombinant fusion proteins

The predicted molecular weights of the Z3-Nluc and Z5-Nluc proteins were 41,870 Da and 54,983 Da, respectively, using the ExPASy Compute pI/MW tool, in agreement with the results of SDS-PAGE (Fig. 1D and E). In addition, MALDI-ToF analyses gave a molecular weight of 41,882 Da for Z3-Nluc protein (Fig. 3A) and 54,865 Da (Fig. 3B) for Z5-Nluc protein, consistent with expectations.

3.3. IgG quantification using SARS-CoV-2 NP or anti-SARS-CoV-2 NP chicken IgY as the capture agent

We evaluated the efficacy of the recombinant Z-Nluc fusion proteins as secondary antibody reporters in a sandwich ELISA format. Each protein demonstrated, as expected, a high affinity for polyclonal human IgG, rabbit IgG, and mouse IgG_{2b} antibodies and insignificant non-specific binding to chicken IgY (Fig. S4A and Fig. S4B). We

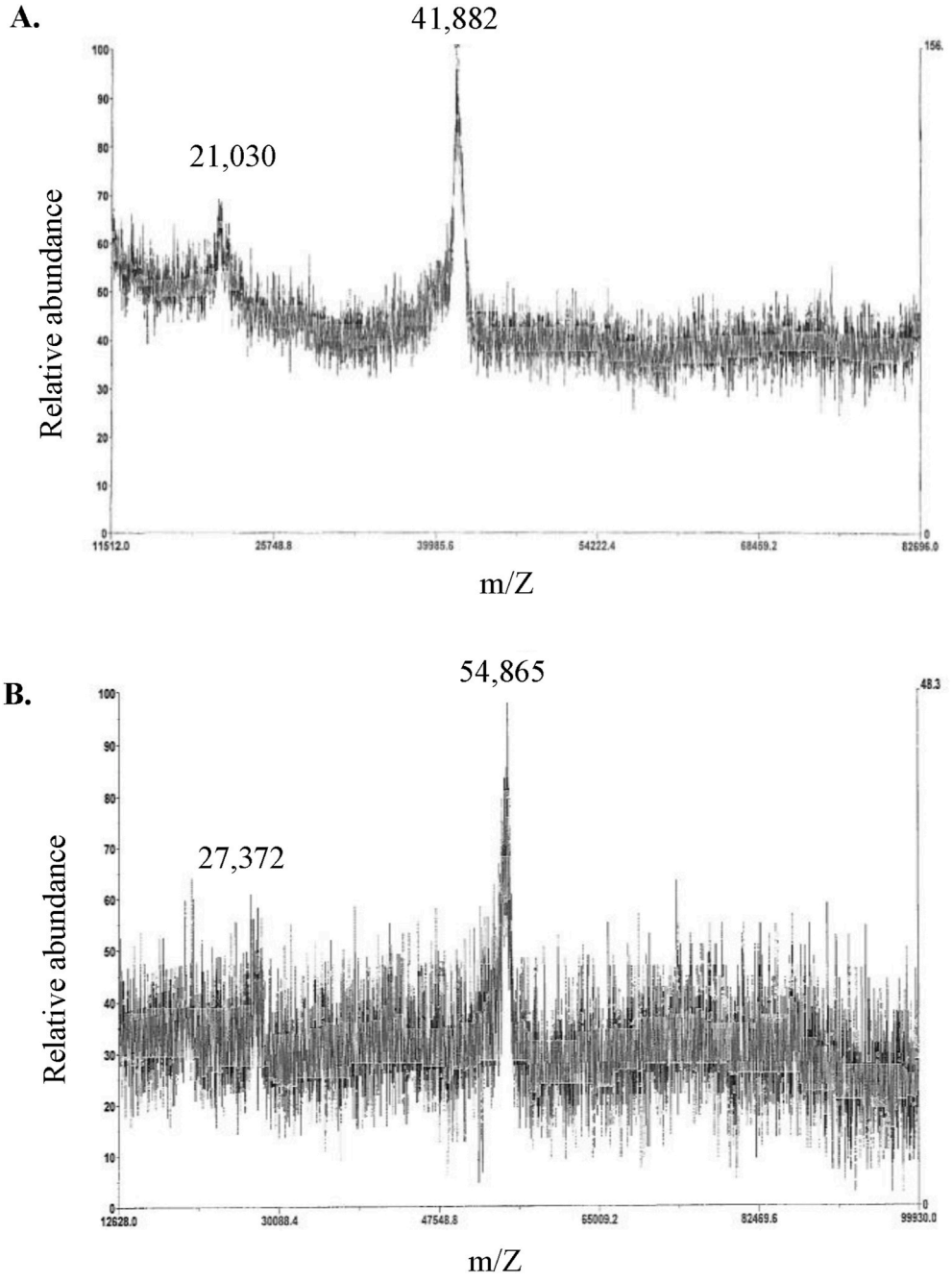

Fig. 3. MALDI-ToF mass spectra of purified recombinant fusion proteins. (A) His_6 tagged Z3-NLuc protein (predicted: 41,870 Da, observed: 41,882 Da, additional prominent peak at 21,030 attributed to the doubly charged ion); (B) His_6 tagged Z5-NLuc protein (predicted: 54,983 Da, observed: 54,865 Da, additional prominent peak at 27,372 attributed to the doubly charged ion). Mass spectrometry analyses was performed in Tufts University Core Facility.

determined an optimal reporter working concentration of 2 μg/ml to ensure that the signal remained below the saturation limit of the Infinite® 200 PRO (Tecan) plate reader (the upper limit was 10^7 RLU; human IgG_1 at concentration> 1000 ng/ml saturates the reader). Although various built-in filters are available to obtain a wider RLU range from the equipment, here we report the RLU signal without a filter to eliminate any filter-based variation. We measured luminescence 3 times from each well at intervals of 4 min and averaged. A sufficient incubation time of the Z-Nluc proteins with antigen-capture antibodies was found to be 60 min, based on our previous interaction kinetics studies.

First, we demonstrated the detection of a mouse anti-SARS-CoV-2 Nucleoprotein (NP) IgG_{2b} (bsm-41411 M, Bioss Antibodies, MA, USA) and a rabbit anti-SARS-CoV-2 NP IgG (NP11H9, Exonbio, CA, USA) in ELISA using SARS-CoV-2 NP as the capture molecule. To investigate the dynamic ranges and sensitivities of assays based on the recombinant proteins, we tested a series of IgG concentrations covering five orders of magnitude (from 10 pg/ml to 1000 ng/ml). With SARS-CoV-2 NP as the capture molecule and Z3-Nluc as the detector, we quantified mouse anti-NP IgG_{2b} with an estimated LOD of 10 pg/ml (Fig. 4A) and a linear dynamic range from 25 pg/mL to 100 ng/mL ($R^2 = 0.98$, Fig. 4A inset). For the rabbit anti-NP IgG with Z3-Nluc as the detector, the LOD was 25 pg/ml (Fig. 4B), and the linear detection range was 50 pg/ml to 50 ng/ml ($R^2 = 0.98$, Fig. 4B inset). In parallel, the Z5-Nluc protein-based assay provided a LOD of 250 pg/ml (Fig. S5A) and a linear range of 50 ng/ml to 500 ng/ml ($R^2 = 0.98$, Fig. S5A inset) for mouse anti-NP IgG_{2b}. Similarly, with the Z5-Nluc, we detected rabbit anti-NP IgG at a LOD of 250 pg/ml (Fig. S5B), and the linear range was 10 ng/ml to 250 ng/ml ($R^2 = 0.98$, Fig. S5B inset).

Next, we used NP on anti-NP polyclonal chicken IgY as the capture molecule in ELISA. We found that LOD with Z3–Nluc was 50 pg/ml (Fig. 4C), and the linear detection range was 500 pg/mL to 500 ng/mL ($R^2 = 0.95$, Fig. 4C inset) for mouse anti-NP IgG_{2b}, and a LOD of 250 pg/ml (Fig. 4D) with a linear range of 500 pg/mL to 100 ng/mL ($R^2 = 0.98$, Fig. 4D inset) for rabbit anti-NP IgG. At the same time, using Z5–Nluc as the detector, a LOD of 250 pg/ml (Fig. S5C) and a linear range of 1 ng/ml to 750 ng/ml ($R^2 = 0.98$, Fig. S5C inset) were obtained for mouse anti-NP IgG_{2b}. For rabbit anti-NP IgG, the LOD with Z5-Nluc was 100 pg/ml (Fig. S5D), and the linear range was from 250 pg/ml to 250 ng/ml ($R^2 = 0.99$, Fig. S5D inset).

The differing analytical performance with mouse and rabbit antibodies can be attributed to the differing affinities of the Z domain for antibodies from different species [37]. Antibodies from various species (mouse [38], guinea pig [39], rabbit [40], cynomolgus monkey [41], hamster [42], donkey [37], dog and cat [43,44], human IgG [9]; with the mouse, hamster, and dog IgGs being the weaker binders) show variable binding affinity with protein A. Also, we generally observed lower LOD values using SARS-CoV-2 NP for capture (10 pg/ml) than when using chicken anti-NP IgY (50 pg/ml). Since some mouse IgG

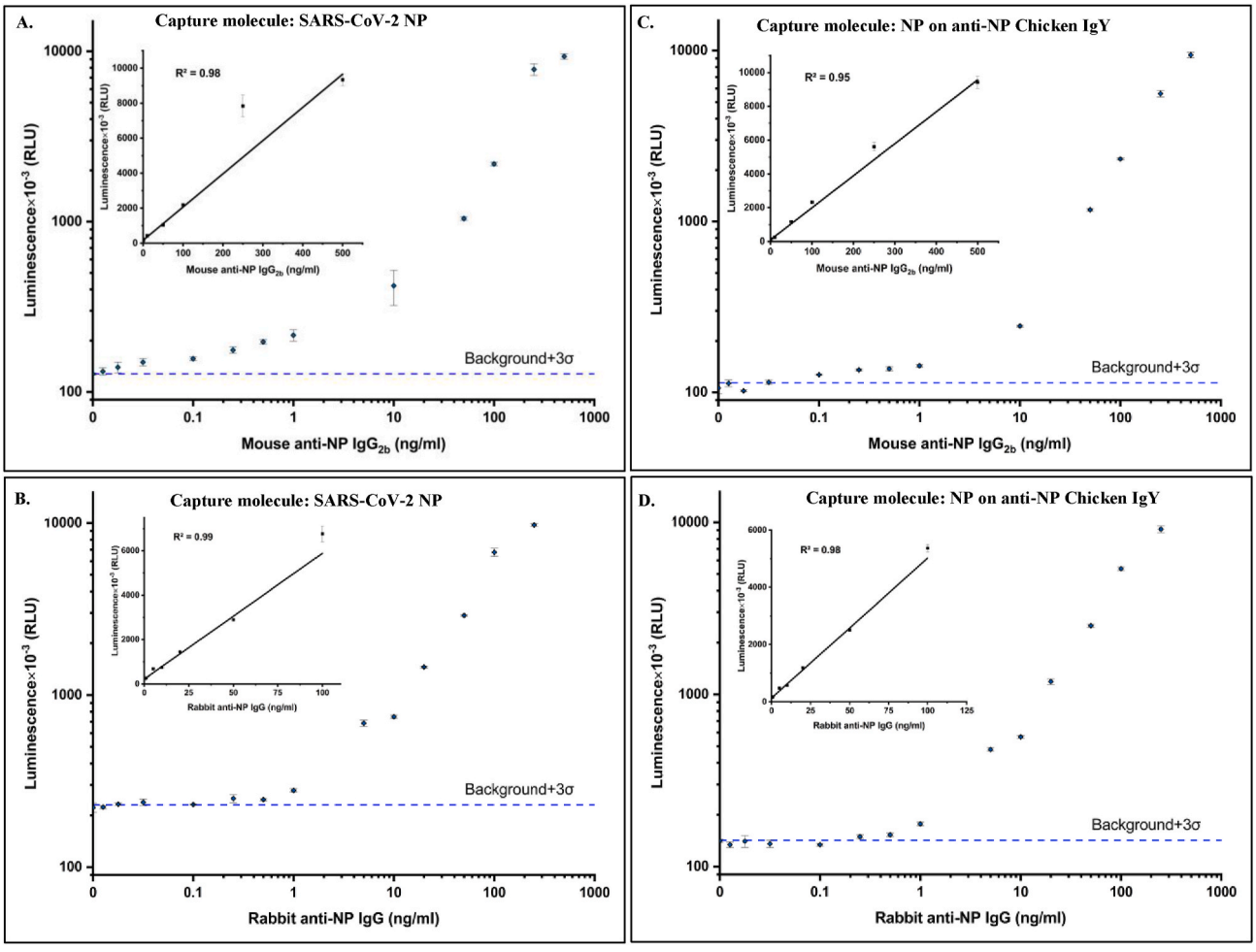

Fig. 4. IgG quantification by Z3–Nluc-ELISA using different capture molecules. Quantification of (A) anti-NP mouse antibodies and (B) anti-NP rabbit antibodies using NP (directly adsorbed on the well) as the capture molecule. Quantification of (C) anti-NP mouse antibodies and (D) anti-NP rabbit antibodies using NP captured on anti-NP chicken IgY as the capture molecule. Each analyte concentration was tested in duplicate wells and each well was measured 3 times; error bars represent the standard deviation of six replicates. The LOD was taken as the intercept with the dashed line representing the average luminescence value of the no-antibody control plus three times the standard deviation (σ) of the no-antibody control (n = 6; σ was 1–7% of the signal).

subclasses do not bind well to protein A, further testing would be needed to validate the assay for different mouse subclasses.

Most importantly, we observed better performance with Z3-Nluc (10 pg/ml) than Z5-Nluc (250 pg/ml) when using NP for capture, possibly due to the difference in the mass fraction of Nluc in the two fusion proteins. Z3-Nluc contains a higher mass fraction of luciferase (46% Nluc for Z3-Nluc and 35% Nluc for Z5-Nluc, by mass) and hence has a higher specific activity. Z5-Nluc, on the other hand, may have an advantage in binding affinity (more Z domain helices would provide more accessible binding sites for IgG Fc binding [15]). Our results are consistent with the affinity of the Z3-Nluc being sufficient to give good assay performance, and in general, we observed better LOD using this molecule (the only exception being the detection of rabbit anti-NP IgG with chicken IgY as capture molecule), presumably because of its higher specific activity.

3.4. IgG detection in human serum

We further assessed the performance of the Z5–Nluc fusion protein (to obtain a wider detection range) with serum (Fig. 5A). Serum assays used medium-binding white polystyrene microplates to reduce non-specific background signals for no-analyte controls (high-binding plates gave high background that interfered with analyte quantification) [45].

We spiked 10% human serum with a dilution series of SARS-CoV-2 NP and quantified the NP on plate-immobilized IgY by adding 1 μg/ml rabbit anti-NP IgG and Z5–Nluc protein. In that format, the Z5–Nluc protein detected the NP with a LOD of 250 pg/ml (25 pg/well) (Fig. 5B). Here, the observed LOD is comparable or superior to previously published luciferase-based immunoassays (LOD of 100 pg/sample for SARS-CoV-2 NP detection using CCD camera) [46]. Separately, we spiked 10% serum with a dilution series of rabbit anti-NP IgG concentrations and quantified the spiked antibody with 2 μg/ml NP captured on plate-immobilized IgY and Z5–Nluc. The LOD for rabbit anti-NP IgG was 100 pg/ml (Fig. 5C). The observed LOD is comparable to those of many anti-SARS-CoV-2 IgG commercial ELISAs, for example: 8 ng/ml (KE30001, Proteintech, IL, USA), 3.9 ng/ml (ABIN6952772, Antibodies-online Inc, PA, USA), 200 pg/ml (ab195215, Abcam, MA, USA).

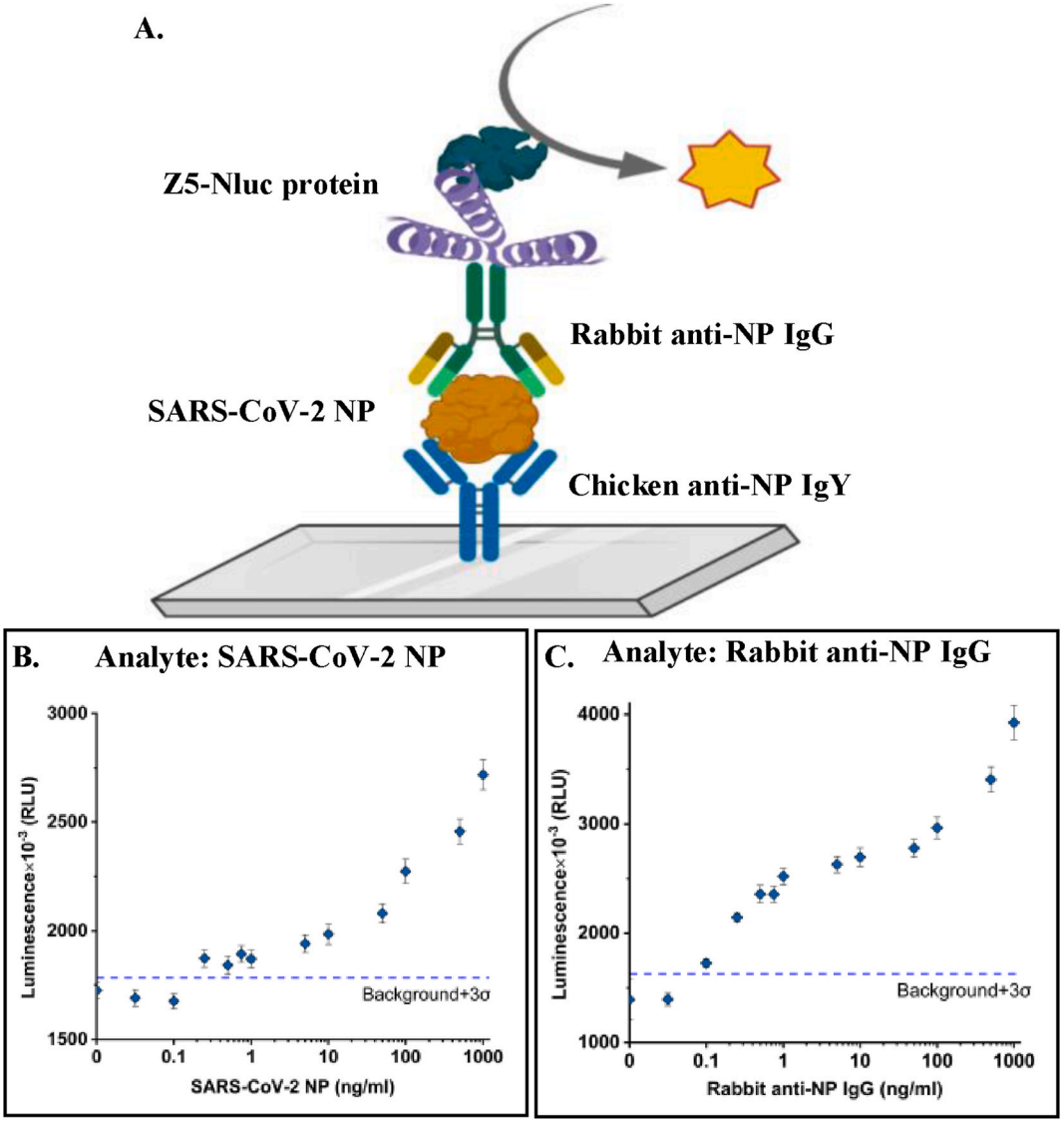

Fig. 5. (A) Schematic of the Z5–Nluc-ELISA used in panels (B) and (C). (B) Detection of SARS-CoV-2 NP spiked in 10% human serum using anti-NP chicken IgY as the capture molecule. (C) Detection of anti-NP rabbit IgG spiked in 10% human serum using NP captured on anti-NP chicken IgY as the capture molecule. The LOD was taken as the intercept with the dashed line representing the average luminescence value of the no-antibody control plus three times the standard deviation (σ) of the no-antibody control.

4. Conclusion

We demonstrated sensitive IgG detection using recombinant fusion proteins comprising multimers of the IgG-binding Z domain of protein A and the ultrabright Nanoluc luciferase. Traditional antibody detection platforms using secondary antibody–reporter conjugates have the drawbacks of low sensitivity and reduced functionality due to steric hindrance from random conjugation [6]. Moreover, a species-specific antibody is needed to design and optimize any antibody detection scheme. The Protein A-Nluc fusion proteins described here detected antibodies of multiple host species in complex fluids containing high protein backgrounds with the selection of appropriate capture molecules. The results indicate that the Z–Nluc fusions may potentially offer a generalized high-sensitivity reporter for assays involving a wide variety of antibodies. Furthermore, we deposited the constructs at Addgene and they are freely available for general use. The Z domain–Nluc fusion proteins provide a generic and flexible platform for sensitive antibody quantification, thereby extending the capabilities of immunochemical analyses.

CRediT authorship contribution statement

Suman Nandy: Conceptualization, Methodology, Validation, Visualization, Investigation. **Mary Crum:** Investigation, Resources. **Katherine Wasden:** Investigation. **Ulrich Strych:** Investigation. **Atul Goyal:** Investigation. **Vijay Maranholkar:** Investigation. **William Mo:** Software. **Binh Vu:** Methodology, Supervision. **Katerina Kourentzi:** Supervision, Funding acquisition, Resources, Writing – review & editing. **Richard C. Willson:** Conceptualization, Supervision, Writing – review & editing, Project administration, Funding acquisition.

Conflicts of Interest

The authors declare no competing interests.

Data availability

Data will be made available on request.

Acknowledgments

We gratefully acknowledge financial support from the CDC (Grant #1U01CK000512-01), NIH/NIAMS (Grant #1R01AR072742-01), DOD CDMRP (Grant #W81XWH-21-1-0975), and NSF (CBET-1928334). In addition, we would like to thank Nam Nguyen, Monish Kumar, and Sayed Golam Mohiuddin from the Department of Chemical and Biomolecular Engineering, University of Houston, for molecular biology training and valuable discussions.

Appendix A. Supplementary data

Supplementary data to this article can be found online at https://doi.org/10.1016/j.ab.2022.114929.

References

[1] L. Zhu, X. Cui, J. Wu, Z. Wang, P. Wang, Y. Hou, M. Yang, Fluorescence immunoassay based on carbon dots as labels for the detection of human immunoglobulin G, Anal. Methods 6 (2014) 4430–4436, https://doi.org/10.1039/C4AY00717D.

[2] H. Zhao, Y. Chang, M. Liu, S. Gao, H. Yu, X. Quan, A universal immunosensing strategy based on regulation of the interaction between graphene and graphene quantum dots, Chem. Commun. 49 (2012) 234–236, https://doi.org/10.1039/C2CC35503E.

[3] H.Y. Song, M.H. Ngai, Z.Y. Song, P.A. MacAry, J. Hobley, M.J. Lear, Practical synthesis of maleimides and coumarin-linked probes for protein and antibody labelling via reduction of native disulfides, Org. Biomol. Chem. 7 (2009) 3400–3406, https://doi.org/10.1039/B904060A.

[4] M. Brinkley, A brief survey of methods for preparing protein conjugates with dyes, haptens and crosslinking reagents, Bioconjugate Chem. 3 (1992) 2–13. https://pubs.acs.org/doi/10.1021/bc00013a001.

[5] B.L. Nilsson, R.J. Hondal, M.B. Soellner, R.T. Raines, Protein assembly by orthogonal chemical ligation methods, J. Am. Chem. Soc. 125 (2003) 5268–5269. https://pubs.acs.org/doi/10.1021/ja029752e.

[6] J.Z. Hui, A.A. Zaki, Z. Cheng, V. Popik, H. Zhang, E.T.L. Prak, A. Tsourkas, Facile method for the site-specific, covalent attachment of full-length IgG onto nanoparticles, Small 10 (2014) 3354–3363, https://doi.org/10.1002/smll.201303629.

[7] J.W. Goding, Use of staphylococcal protein A as an immunological reagent, J. Immunol. Methods 20 (1978) 241–253, https://doi.org/10.1016/0022-1759(78)90259-4.

[8] M. Ultsch, A. Braisted, H.R. Maun, C. Eigenbrot, 3-2-1: structural insights from stepwise shrinkage of a three-helix Fc-binding domain to a single helix, Protein Eng. Des. Sel. 30 (2017) 619–625, https://doi.org/10.1093/protein/gzx029.

[9] J. Deisenhofer, Crystallographic refinement and atomic models of a human Fc fragment and its complex with fragment B of protein A from *Staphylococcus aureus* at 2.9- and 2.8-Å resolution, Biochemistry 20 (1981) 2361–2370, https://doi.org/10.1021/bi00512a001.

[10] H. Gouda, M. Shiraishi, H. Takahashi, K. Kato, H. Torigoe, Y. Arata, I. Shimada, NMR study of the interaction between the B domain of staphylococcal protein A and the Fc portion of immunoglobulin G, Biochemistry 37 (1998) 129–136, https://doi.org/10.1021/bi970923f.

[11] L. Cedergren, R. Andersson, B. Jansson, M. Uhlén, B. Nilsson, Mutational analysis of the interaction between staphylococcal protein a and human IgG1, Protein Eng. Des. Sel. 6 (1993) 441–448, https://doi.org/10.1093/protein/6.4.441.

[12] B. Nilsson, T. Moks, B. Jansson, L. Abrahmsén, A. Elmblad, E. Holmgren, C. Henrichson, T.A. Jones, M. Uhlén, A synthetic IgG-binding domain based on staphylococcal protein a, Protein Eng. Des. Sel. 1 (1987) 107–113, https://doi.org/10.1093/protein/1.2.107.

[13] B. Madan, G. Chaudhary, S.M. Cramer, W. Chen, ELP-z and ELP-zz capturing scaffolds for the purification of immunoglobulins by affinity precipitation, J. Biotechnol. 163 (2013) 10–16, https://doi.org/10.1016/J.JBIOTEC.2012.10.007.

[14] M. Eliasson, A. Olsson, E. Palmcrantz, K. Wiberg, M. Inganäs, B. Guss, M. Lindberg, M. Uhlén, Chimeric IgG-binding receptors engineered from staphylococcal protein A and streptococcal protein G, J. Biol. Chem. 263 (1988) 4323–4327, https://doi.org/10.1016/S0021-9258(18)68928-8.

[15] L. Jendeberg, B. Persson, R. Andersson, R. Karlsson, M. Uhlén, B. Nilsson, Kinetic analysis of the interaction between protein a domain variants and human Fc using plasmon resonance detection, J. Mol. Recogn. 8 (1995) 270–278, https://doi.org/10.1002/JMR.300080405.

[16] U. Patil, M. Crum, B. Vu, K. Wasden, K. Kourentzi, R.C. Willson, Continuous Fc detection for protein A capture process control, Biosens. Bioelectron. 165 (2020), 112327, https://doi.org/10.1016/j.bios.2020.112327.

[17] E. Kobatake, T. Iwai, Y. Ikariyama, M. Aizawa, Bioluminescent immunoassay with a protein A-luciferase fusion protein, Anal. Biochem. 208 (1993) 300–305, https://doi.org/10.1006/ABIO.1993.1050.

[18] M. Mie, N.P.B. Thuy, E. Kobatake, Development of a homogeneous immunoassay system using protein A fusion fragmented Renilla luciferase, Analyst 137 (2012) 1085–1089, https://doi.org/10.1039/c2an15976g.

[19] C. Lindbladh, K. Mosbach, L. Bülow, Preparation of a genetically fused protein A/luciferase conjugate for use in bioluminescent immunoassays, J. Immunol. Methods 137 (1991) 199–207, https://doi.org/10.1016/0022-1759(91)90025-b.

[20] X.M. Zhang, E. Kobatake, K. Kobayashi, Y. Yanagida, M. Aizawa, Genetically fused protein A-luciferase for immunological blotting analyses, Anal. Biochem. 282 (2000) 65–69, https://doi.org/10.1006/ABIO.2000.4584.

[21] T. Ebihara, H. Takayama, Y. Yanagida, E. Kobatake, M. Aizawa, Thermostabilization of protein A-luciferase fusion protein by single amino acid mutation, Biotechnol. Lett. 24 (2002) 147–149, https://doi.org/10.1023/A:1013858814175.

[22] M. Nakamura, M. Mie, E. Kobatake, Construction of a functional IgG-binding luciferase fusion protein for the rapid detection of specific bacterial strains, Analyst 136 (2011) 71–72, https://doi.org/10.1039/c0an00460j.

[23] A. Farzannia, R. Roghanian, S.H. Zarkesh-Esfahani, M. Nazari, R. Emamzadeh, FcUni-RLuc: an engineered Renilla luciferase with Fc binding ability and light emission activity, Analyst 140 (2015) 1438–1441, https://doi.org/10.1039/c4an01946f.

[24] M.P. Hall, J. Unch, B.F. Binkowski, M.P. Valley, B.L. Butler, M.G. Wood, P. Otto, K. Zimmerman, G. Vidugiris, T. Machleidt, M.B. Robers, H.A. Benink, C.T. Eggers, M.R. Slater, P.L. Meisenheimer, D.H. Klaubert, F. Fan, L.P. Encell, K.V. Wood, Engineered luciferase reporter from a deep sea shrimp utilizing a novel imidazopyrazinone substrate, ACS Chem. Biol. 7 (2012) 1848–1857, https://doi.org/10.1021/cb3002478.

[25] H. Oyama, Y. Kiguchi, I. Morita, T. Miyashita, A. Ichimura, H. Miyaoka, A. Izumi, S. Terasawa, N. Osumi, H. Tanaka, T. Niwa, N. Kobayashi, NanoLuc luciferase as a suitable fusion partner of recombinant antibody fragments for developing sensitive luminescent immunoassays, Anal. Chim. Acta 1161 (2021), 238180, https://doi.org/10.1016/j.aca.2020.12.055.

[26] T. Alsulami, N. Nath, R. Flemming, H. Wang, W. Zhou, J.-H. Yu, Development of a novel homogeneous immunoassay using the engineered luminescent enzyme NanoLuc for the quantification of the mycotoxin fumonisin B1, Biosens. Bioelectron. 177 (2021), 112939, https://doi.org/10.1016/j.bios.2020.112939.

[27] Y. Liang, H. Yan, L. Huang, J. Zhao, H. Wang, M. Kang, Z. Wan, J. Shui, S. Tang, A luciferase immunosorbent assay for quantitative detection of IgG antibodies

against SARS-CoV-2 nucleoprotein, J. Virol. Methods 292 (2021), 114141, https://doi.org/10.1016/j.jviromet.2021.114141.
[28] D. Katz, S. Lehrer, A. Kohn, Use of chicken and rabbit antibodies in a solid phase protein a radioimmunoassay for virus detection, J. Virol. Methods 12 (1985) 59–70, https://doi.org/10.1016/0166-0934(85)90008-4.
[29] A. Larsson, J. Sjöquist, Chicken IgY: utilizing the evolutionary difference, Comp. Immunol. Microbiol. Infect. Dis. 13 (1990) 199–201, https://doi.org/10.1016/0147-9571(90)90088-B.
[30] R.P.D. Bank, RCSB PDB - 2SPZ: staphylococcal protein A, Z-domain, NMR, 10 structures (n.d.), https://www.rcsb.org/structure/2SPZ. (Accessed 28 October 2021).
[31] S. Lovell, N. Mehzabeen, K.P. Battaile, M.G. Wood, L.P. Encell, K.V. Wood, 1.95 A resolution structure of NanoLuc luciferase, RCSB protein Data Bank PDB ID, 5IBO (2016), https://doi.org/10.2210/pdb5ibo/pdb, 1.
[32] H.M. Berman, J. Westbrook, Z. Feng, G. Gilliland, T.N. Bhat, H. Weissig, I. N. Shindyalov, P.E. Bourne, The protein Data Bank, Nucleic Acids Res. 28 (2000) 235–242, https://doi.org/10.1093/nar/28.1.235.
[33] L.A. Kelley, S. Mezulis, C.M. Yates, M.N. Wass, M.J.E. Sternberg, The Phyre2 web portal for protein modeling, prediction and analysis, Nat. Protoc. 10 (2015) 845–858, https://doi.org/10.1038/nprot.2015.053.
[34] S. Nakamura, N. Fu, K. Kondo, K.-I. Wakabayashi, T. Hisabori, K. Sugiura, A luminescent Nanoluc-GFP fusion protein enables readout of cellular pH in photosynthetic organisms, J. Biol. Chem. 296 (2021), 100134, https://doi.org/10.1074/jbc.RA120.016847.
[35] S.F.A. Wouters, W.J.P. Vugs, R. Arts, N.M. de Leeuw, R.W.H. Teeuwen, M. Merkx, Bioluminescent antibodies through photoconjugation of protein G–luciferase fusion proteins, Bioconjugate Chem. 31 (2020) 656–662, https://doi.org/10.1021/acs.bioconjchem.9b00804.
[36] N. Boute, P. Lowe, S. Berger, M. Malissard, A. Robert, M. Tesar, NanoLuc luciferase – a multifunctional tool for high throughput antibody screening, Front. Pharmacol. 7 (2016) 27, https://doi.org/10.3389/fphar.2016.00027.
[37] C. Chen, Q.-L. Huang, S.-H. Jiang, X. Pan, Z.-C. Hua, Immobilized protein ZZ, an affinity tool for immunoglobulin isolation and immunological experimentation, Biotechnol. Appl. Biochem. 45 (2006) 87–92, https://doi.org/10.1042/BA20060055.
[38] P.L. Ey, S.J. Prowse, C.R. Jenkin, Isolation of pure IgG_1, IgG_{2a} and IgG_{2b} immunoglobulins from mouse serum using protein A-Sepharose, Mol. Immunol. 15 (1978) 429–436, https://doi.org/10.1016/0161-5890(78)90070-6.
[39] L.N. Martin, Separation of Guinea pig IgG subclasses by affinity chromatography on protein A-Sepharose, J. Immunol. Methods 52 (1982) 205–212, https://doi.org/10.1016/0022-1759(82)90046-1.
[40] N.L. Brown, S.P. Bottomley, M.D. Scawen, M.G. Gore, A study of the interactions between an IgG-binding domain based on the B domain of staphylococcal protein A and rabbit IgG, Mol. Biotechnol. 10 (1998) 9–16, https://doi.org/10.1007/BF02745859.
[41] H. Liu, A.V. Manuilov, C. Chumsae, M.L. Babineau, E. Tarcsa, Quantitation of a recombinant monoclonal antibody in monkey serum by liquid chromatography–mass spectrometry, Anal. Biochem. 414 (2011) 147–153, https://doi.org/10.1016/j.ab.2011.03.004.
[42] J.E. Coe, P.R. Coe, M.J. Ross, Staphylococcal protein a purification of rodent IgG_1 and IgG_2 with particular emphasis on Syrian hamsters, Mol. Immunol. 18 (1981) 1007–1012, https://doi.org/10.1016/0161-5890(81)90119-X.
[43] M.A. Scott, J.M. Davis, K.A. Schwartz, Staphylococcal protein A binding to canine IgG and IgM, Vet. Immunol. Immunopathol. 59 (1997) 205–212, https://doi.org/10.1016/S0165-2427(97)00073-1.
[44] Z. Peng, F. Estelle, R. Simons, A.B. Becker, Differential binding properties of protein A and protein G for dog immunoglobulins, J. Immunol. Methods 145 (1991) 255–258, https://doi.org/10.1016/0022-1759(91)90335-D.
[45] D.E. Rebeski, E.M. Winger, Y.K. Shin, M. Lelenta, M.M. Robinson, R. Varecka, J. R. Crowther, Identification of unacceptable background caused by non-specific protein adsorption to the plastic surface of 96-well immunoassay plates using a standardized enzyme-linked immunosorbent assay procedure, J. Immunol. Methods 226 (1999) 85–92, https://doi.org/10.1016/S0022-1759(99)00051-4.
[46] V.R. Viviani, J.R. Silva, P.L. Ho, A novel brighter bioluminescent fusion protein based on ZZ domain and amydetes vivianii firefly luciferase for immunoassays, Front. Bioeng. Biotechnol. 9 (2021), 755045, https://doi.org/10.3389/fbioe.2021.755045.